

# Electronic Supplementary Information

## Synthesis of Nickel Hexacyanoferrate Nanocubes with Tuneable Dimensions via Temperature-Controlled Ni<sup>2+</sup>-Citrate Complexation.

Sascha Keßler,<sup>a</sup> Guillermo González-Rubio,<sup>a</sup> Elrike Reinalter,<sup>a</sup> Michael Kovermann<sup>a</sup> and Helmut Cölfen<sup>a</sup>

<sup>a</sup>. *Physical Chemistry, Department of Chemistry, University of Konstanz, Universitätsstrasse 10, D-78457 Konstanz, Germany.*

### 1. Materials and Methods

**Materials:** Potassium hexacyanoferrate(III) (98.0 %) was purchased from Alfa Aesar. Nickel(II) acetate tetrahydrate (99.0 %), trisodium citrate (≥99.0 %) and deuterium oxide (99.9 %) were purchased from Sigma Aldrich. Chloroform (Stabilized with 0.6 % ethanol) was purchased from VWR Chemicals. All aqueous solutions were prepared by using deionized Milli Q water (18.2 mΩ cm<sup>-1</sup>) obtained from a Milli Q Direct-8 system.

**NiHCF NC synthesis.** Potassium hexacyanoferrate(III) (0.262 g, 0.794 mmol) was dissolved in 40 mL of water and injected (20.0 mL min<sup>-1</sup>) into 40 mL of nickel(II) acetate tetrahydrate (0.298 g, 1.198 mmol) and trisodium citrate dihydrate (0.528 g, 1.796 mmol) aqueous solution. The reaction was carried out in a double-walled reaction vessel equipped with a cryostat to enable temperature control (0 °C, 10 °C, 25 °C, 35 °C, 50 °C, 70 °C or 90 °C). The mixture was left under stirring for 24 and then centrifuged at 7000 rpm for 10 minutes. The supernatant was discarded, and the precipitated nanoparticles were rinsed with water (4 x 30 mL). Subsequently, they were redispersed in water (Vortex mixer) and the centrifugation step was repeated at least three times. The resulting orange solid was dried in a vacuum oven at 40 °C for a day.

**Mesocrystal Formation:** A double-polished silicon wafer was placed inside a small glass tube (1.0 mL, 3.5 mm x 8.0 mm). The NiHCF NCs were dispersed in water to form a dispersion (5.0 mg mL<sup>-1</sup>). 0.6 mL of the NiHCF dispersion was added to the glass tube. This glass tube was placed in a small glass vial. 0.8 mL of ethanol was added to the glass vial to induce the gas-phase diffusion experiment. The crystallization process took 14 days. The mesocrystals were harvested by removing the supernatant with a syringe followed by transferring the silicon wafer onto a filter paper for drying.

**Titration experiments:** An automated commercially available titration setup (a 905 Titrand and two 800 Dosino dosing units) provided by Metrohm and operated with the custom-made software Tiamo 2.3 was used. Conductivity was recorded using a cell Metrohm (6.0910.120) equipped with a conductivity module 856 Metrohm (2.856.0010). For pH measurements, a flat membrane pH electrode provided by Metrohm (6.0269.100) was used. In a typical titration experiment, 42 mL of an aqueous solution of 0.1 M nickel(II) acetate tetrahydrate was added ( $0.05 \text{ mL min}^{-1}$ ) into 40 mL of an aqueous trisodium citrate solution: 0.01 M, 0.025 M or 0.05 M.

**Turbidity measurements:** An optrode sensor (6.1115.000) equipped with a 660 nm laser was used (Metrohm).

**NMR spectra:** All experiments were carried out using a Bruker Avance III 600 spectrometer.  $^1\text{H}$  chemical shifts are given in ppm and referenced to the solvent signals. A relaxation delay of 1.0 s and an acquisition time of 2.7 s were typically employed. However, for in-situ monitoring of the NiHFC growth, a relaxation delay of 20.0 s and an acquisition time of 2.7 s were used. A relaxation delay of 5.0 s, a pi-pulse of approximately 20  $\mu\text{s}$  (varied between 17.5  $\mu\text{s}$  and 22.7  $\mu\text{s}$ ) and an acquisition time of 0.26 s were employed during the Carr-Purcell-Meiboom-Gill (CPMG) experiments. In terms of citrate, approximately 20 sets of loops between 4 and 1100 repetitions were used. For the complex, a set of 12 different loops between 4 and 1100 repetitions were used. All data were processed and analyzed with MestReNova and Topspin software.

- *NiHFC growth.* 0.3 mL of an aqueous ( $\text{D}_2\text{O}$ ) potassium hexacyanoferrate(III) solution (0.020 M) was rapidly added to 0.3 mL of an aqueous ( $\text{D}_2\text{O}$ ) solution of nickel(II) acetate tetrahydrate (0.030 M) and trisodium citrate dihydrate (0.045 M).
- *Determination of  $\text{Ni}^{2+}$ -Citrate Stoichiometry.* Trisodium citrate was dissolved in 0.4 mL of deuterium oxide to obtain a concentration of 0.05 M, and a certain volume of a 0.1 M nickel acetate solution in deuterium oxide was added. After each addition, the  $^1\text{H}$ -NMR of the mixture was immediately recorded.

**Isothermal Titration Calorimetry:** All experiments were performed with a Micorcal ITC200 system from Malvern. The data were analyzed using NITPIC (The University of Texas Southwestern Medical Centre) and ITCsy (sedphat) software. The plots were processed with GUSSI (The University of Texas Southwestern Medical Centre) and Origin 2017. The experiment was performed for each titration in triplicates unless explicitly stated otherwise.

**Electron Microscopy:** Transmission electron microscopy images were obtained in a Zeiss Libra 120 EF-TEM operating at an acceleration voltage of 120 kV. Nanoparticles were drop casted on carbon-

coated 400 square mesh copper grid. Scanning electron microscopy images were recorded with an Auriga 40 by Zeiss operating at 5 kV. Energy-dispersive X-ray spectroscopy (EDS) was applied by a Gemini 500 by Zeiss operating at 10 kV. For EDS measurement, the nanoparticle dispersion was drop casted on a double-polished Si-wafer. Afterwards, the dried sample was coated by a gold film (thickness of approximately 4.0 nm).

**Powder X-ray diffraction:** All samples were characterized using a Bruker D8 Advance equipped with a scintillation counter, and a Bruker D8 Discovery with a Lynxeye XE detector. For the WAXS measurement a Vantec detector was used.

**Thermogravimetric analysis:** The sample was analyzed using a NETZSCH STA449 F3 Jupiter. All measurements were performed using a gas flow of air ( $254 \text{ mL min}^{-1}$ ) and nitrogen ( $250 \text{ mL min}^{-1}$ ). Heating rates of  $5 \text{ K min}^{-1}$  in the range between  $30 \text{ }^\circ\text{C}$  and  $300 \text{ }^\circ\text{C}$  and  $10 \text{ K min}^{-1}$  in the range between  $300 \text{ }^\circ\text{C}$  and  $1000 \text{ }^\circ\text{C}$  were applied.

## 2. Nickel hexacyanoferrate crystal structure and composition

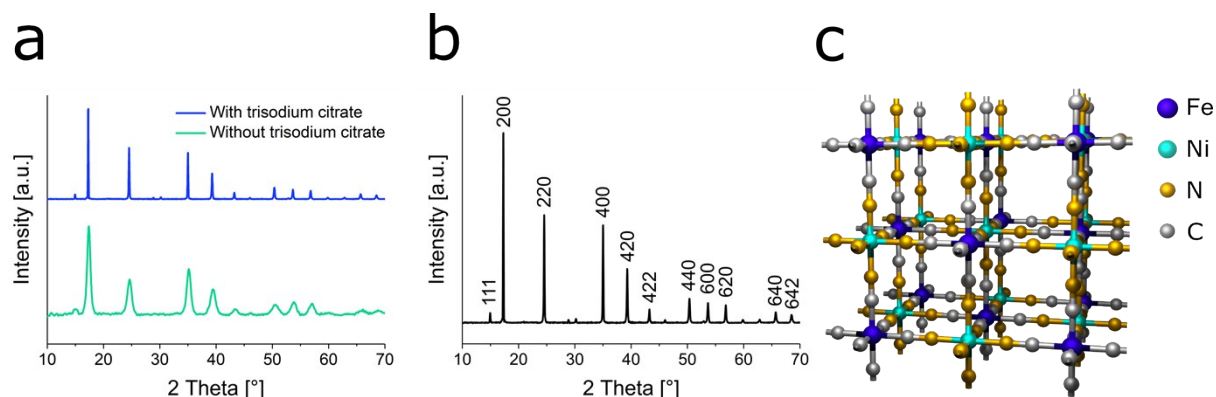


**Figure S1.** (a) Normalized PXRD patterns of NiHCF nanoparticles prepared in the absence (green curve) and presence (blue curve) of trisodium citrate. (b) Assigned PXRD pattern of NiHCF NCs prepared in the presence of trisodium citrate (reference: file JCP2.2CA: 01-082-2283). (c) Unit cell of nickel hexacyanoferrate. Color code: blue, iron(III); green, nickel(II); yellow, nitrogen; grey, carbon.

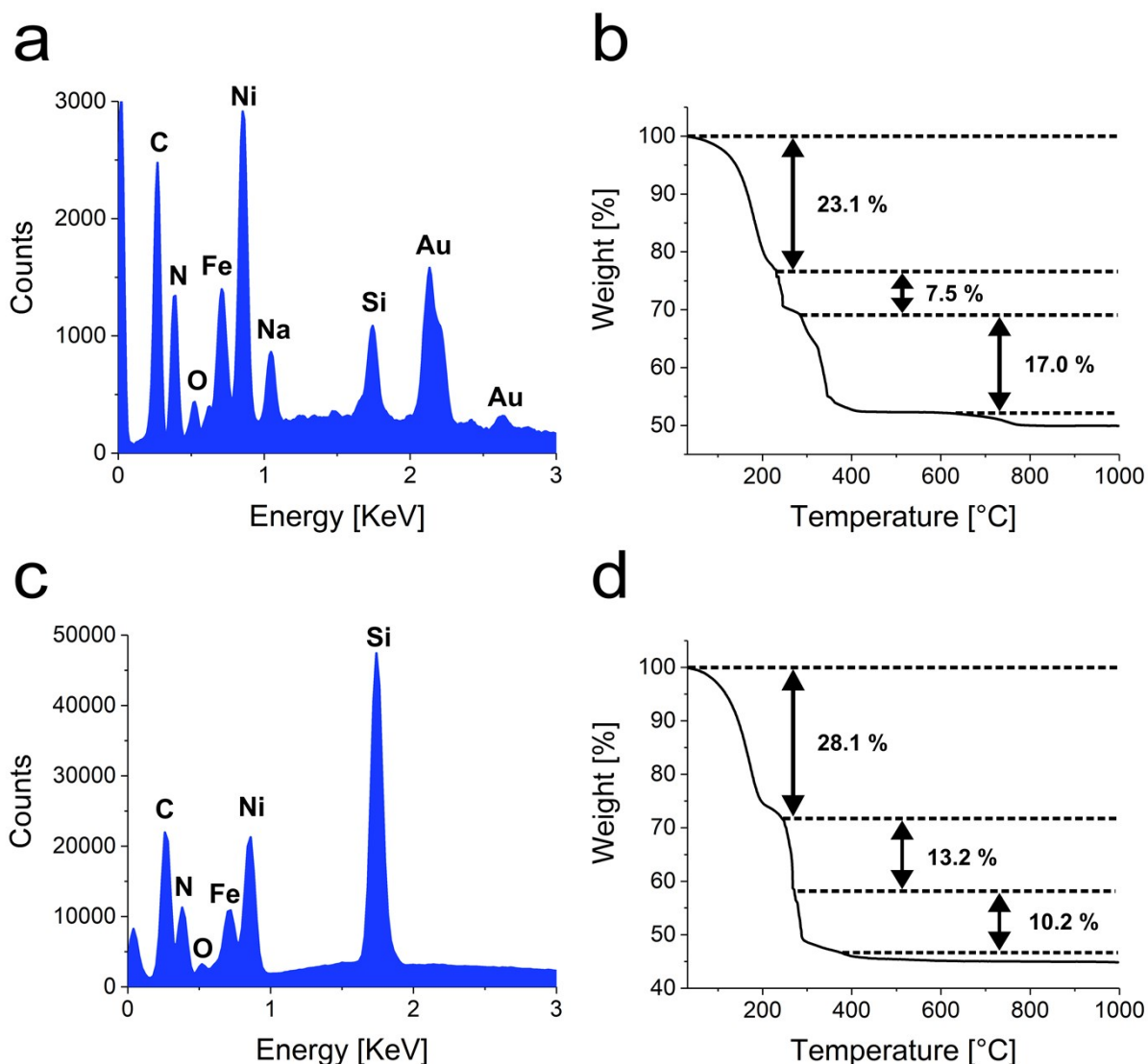


**Figure S2.** (a) EDS spectrum of NiHCF NCs synthesized in the presence of citrate. The [Na]:[Ni]:[Fe] ratio was determined to be 0.125:2.875:2.000. The signals for silicon and gold can be assigned to used Si-wafer and the gold coating. (b) Thermogravimetric analysis (TGA) curve of the corresponding NiHCF NCs in air. The first two processes show a weight loss due to evaporation of water molecules attached to the nanocubes. Thereby, an amount of 14.7 mol per 1.0 mol of NiHCF was determined. The third process appeared due to the decomposition of the cyano-bridged framework.<sup>1</sup> The fourth process can be assigned to formation of metal oxides. (c) EDS spectrum of NiHCF NCs synthesized in the absence of citrate. The [K]:[Ni]:[Fe] ratio was determined to be 0.14:2.86:2.00. The signal for silicon can be assigned to the used Si-wafer. (d) Corresponding thermogravimetric analysis (TGA) curve of NiHCF NCs in air. The first two processes show a weight loss due to evaporation of water molecules attached to the NCs. Thereby, an amount of 23.5 mol per 1.0 mol of NiHCF was obtained. The third process occurred due to the decomposition framework.<sup>1</sup> The fourth process can be assigned to formation of metal oxides.

**Table S1.** EDS data of the NiHCF NCs synthesized in presence and absence of citrate. Note that carbon and nitrogen were not included in the composition calculation, as the data of light elements are not representative for a quantitative calculation. The oxygen content can be attributed to the presence of water molecules attached to the NCs.

Element	Synthesized in presence of citrate		Synthesized in absence of citrate	
	Wt%	$\sigma$ Wt%	Wt%	$\sigma$ Wt%
C	22.09	0.34	25.50	0.37
N	21.37	0.30	18.62	0.23
Na	2.66	0.08	0.00	0.00
K	0.00	0.00	2.27	0.18
Fe	21.25	0.44	20.58	0.09
Ni	30.55	0.33	30.90	0.36
O	2.08	0.09	2.14	0.08

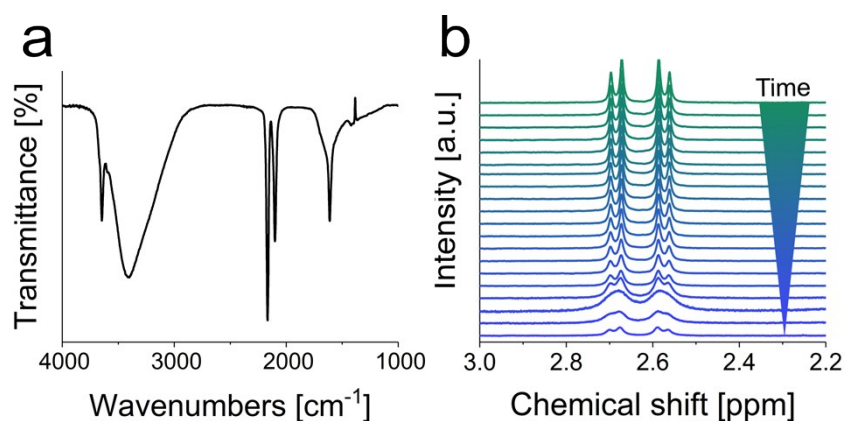


**Figure S3.** (a) IR-spectrum of NiHCF NCs (transmission mode). The signals at 1612 and 3405  $\text{cm}^{-1}$  are assigned to interstitial water, while that one at 3648  $\text{cm}^{-1}$  is attributed to the hydroxyl groups on the surface. The intense signals at 2167  $\text{cm}^{-1}$  and 2101  $\text{cm}^{-1}$  correspond, respectively, to the stretching vibration band and bridging isomer of the cyano-groups ( $\text{C}\equiv\text{N}$ ) coordinated to both,  $\text{Ni}^{2+}$  and  $\text{Fe}^{2+}$ .<sup>2</sup> (b)  $^1\text{H}$ -NMR spectra of trisodium citrate proton signals during the standard NiHCF NCs synthesis in  $\text{D}_2\text{O}$  (time scale: 24 h, color-coded from blue to green).

### 3. pH of the Growth Solution

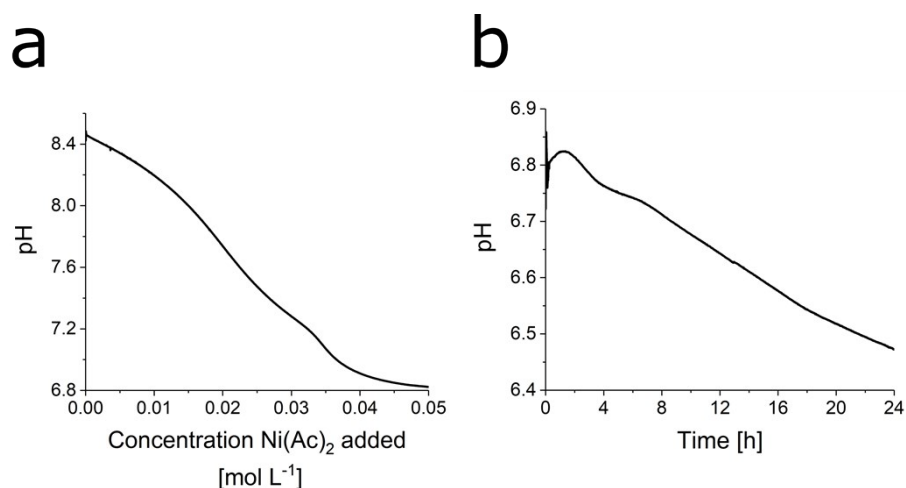


**Figure S4.** (a) Trisodium citrate solution (0.01 M) pH evolution as a function of the concentration of nickel acetate (0.1 M) at 25 °C. (b) pH variation during the synthesis of NiHFC NCs in the presence of citrate at 25 °C.

### 4. Determination of Ni<sup>2+</sup>-Citrate Stoichiometry

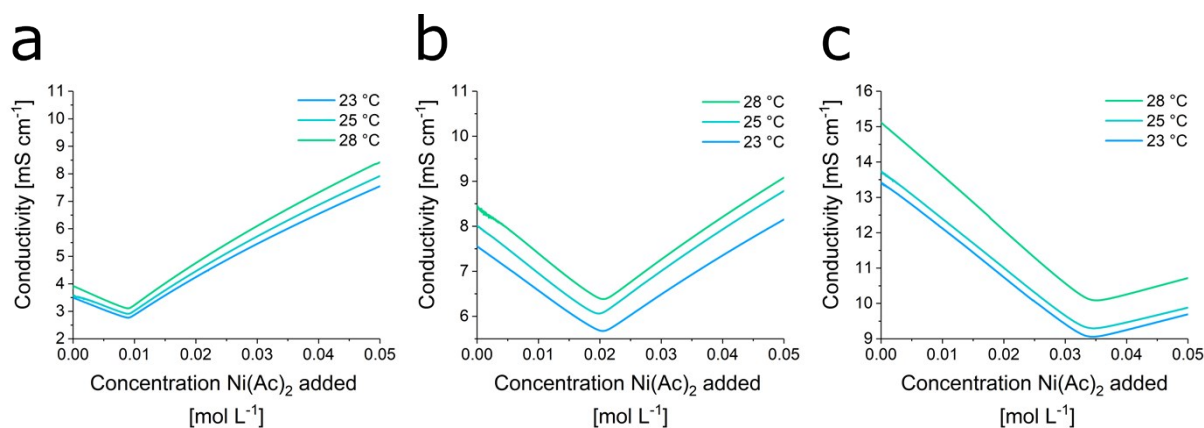


**Figure S5.** Conductometric titration curves: The addition of an aqueous nickel acetate solution (0.1 M) into aqueous trisodium citrate solutions ((a) 0.01 M, (b) 0.025 M, (c) 0.05 M) at different temperatures (Addition rate: 0.05 mL min<sup>-1</sup>). During the addition of nickel acetate, the conductivity of the trisodium citrate solution decreased due to the formation of a Ni<sup>2+</sup>-citrate complex. Once all citrate molecules are chelating Ni<sup>2+</sup> (equivalence point), further addition of nickel(II) acetate lead to a rise of the conductivity. The binding ratios were derived from the equivalence point (Table S2).

**Table S2.** Binding ratios of  $\text{Ni}^{2+}$  with citrate obtained from the conductometric titration curves at different temperatures (23 °C, 25 °C and 28 °C) and citrate concentrations.

Temperature [°C]	0.01 M trisodium citrate solution	0.025 M trisodium citrate solution	0.05 M trisodium citrate solution
23	1.05	1.03	0.99
25	1.06	0.99	0.99
28	1.08	1.03	0.99

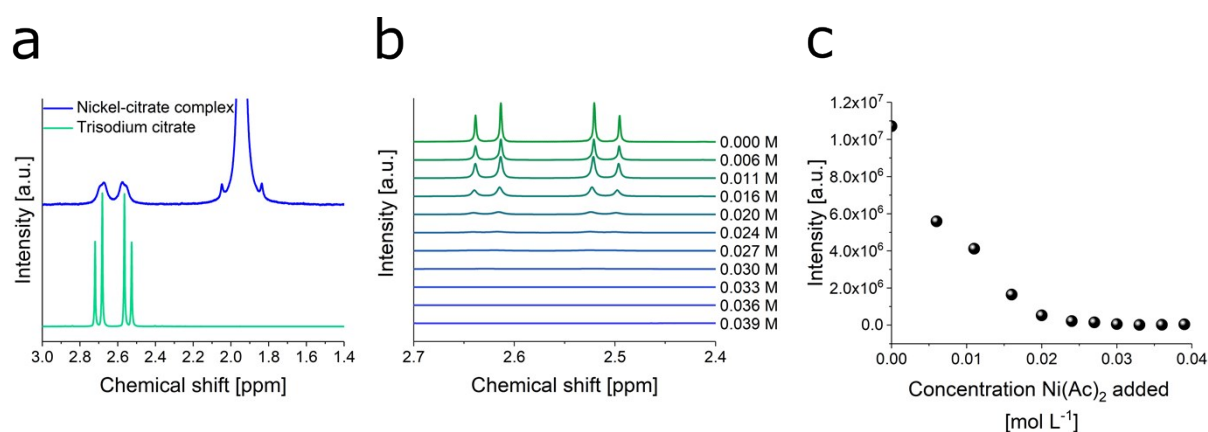


**Figure S6.** (a)  $^1\text{H-NMR}$  spectra of trisodium citrate in the absence (green) and presence (blue) trisodium of  $\text{Ni}^{2+}$  ([citrate]:[ $\text{Ni}^{2+}$ ]= 1.5 ). (b) Evolution of citrate  $^1\text{H-NMR}$  spectra during the addition of  $\text{Ni}^{2+}$ . (c) Evolution of the citrate  $^1\text{H-NMR}$  signal at 2.61 ppm during the addition of  $\text{Ni}^{2+}$

## 5. Growth kinetics in the absence and presence of citrate at 25 °C

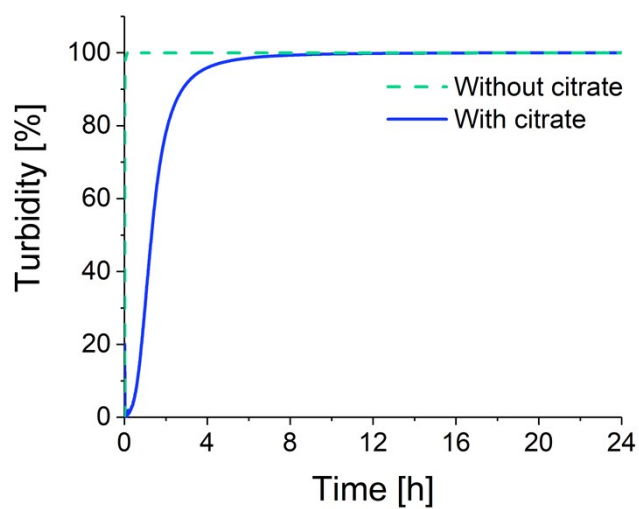


**Figure S7.** Time course of the turbidity during the synthesis of NiHCF in the absence (green color) and presence (blue color) of citrate at 25 °C.

## 6. Size dispersity of NiHCF NCs obtained at different temperatures

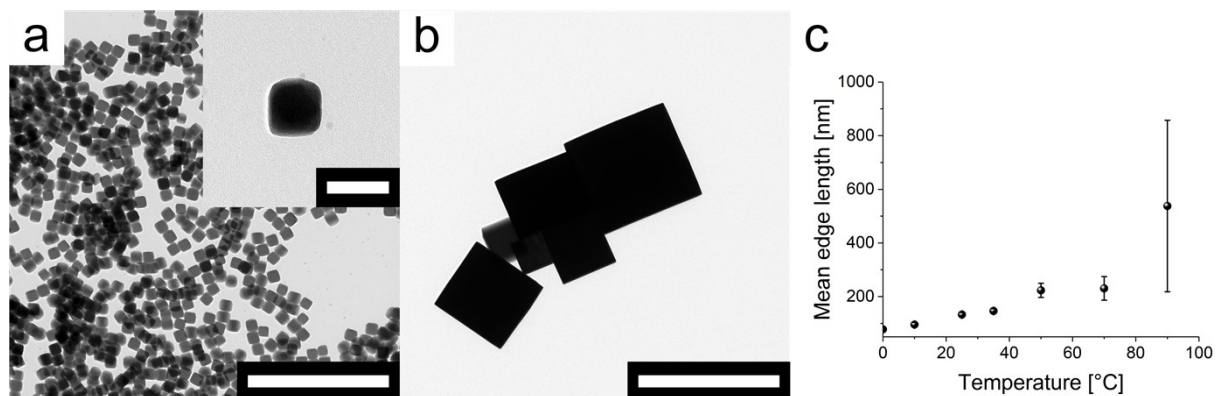


**Figure S8.** TEM micrographs of NiHCF with distinct dimensions: (a)  $78 \pm 4.9$  nm at 0 °C and (b)  $538 \pm 320$  nm at 90 °C. Scale bars: 1 μm and 100 nm (Insets). (c) Temperature-dependent mean edge length evolution of NiHCF NCs. Data derived from TEM micrographs of NiHCF NCs obtained with distinct dimensions:  $78 \pm 4.9$  nm at 0 °C,  $96 \pm 8.3$  nm at 10 °C,  $133 \pm 8.0$  nm at 25 °C,  $147 \pm 8.0$  nm at 35 °C,  $223 \pm 26$  nm at 50 °C,  $231 \pm 44$  nm at 70 °C (200 NCs counted) and  $538 \pm 320$  nm at 90 °C (20 NCs counted). Size dispersity below 8 % between 10 °C and 35 °C, 12 % at 50 °C, 20 % at 70 °C and 59 % at 90 °C.

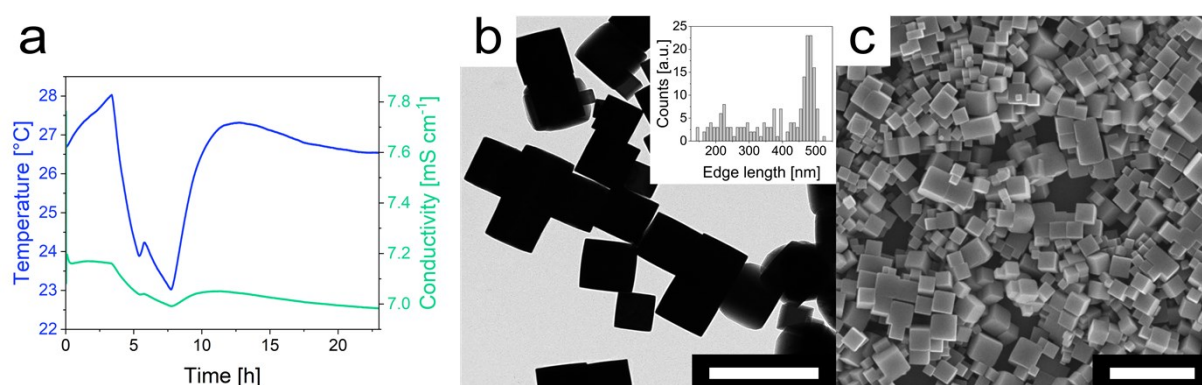


**Figure S9.** NiHCF nanocrystal growth in the absence of temperature control. (a) Conductivity measurement during the synthesis of NiHCF NCs in the absence (green curve) of temperature control. Temperature oscillations during the synthesis measured by the conductivity electrode (blue curve) (b) TEM and (c) SEM images of the obtained NiHCF NCs (inset b: NiHCF NC edge length distribution; 200 NCs counted). Scale bars: 1.0 μm

## 7. Investigation of the temperature-dependent Ni<sup>2+</sup>-citrate complexation

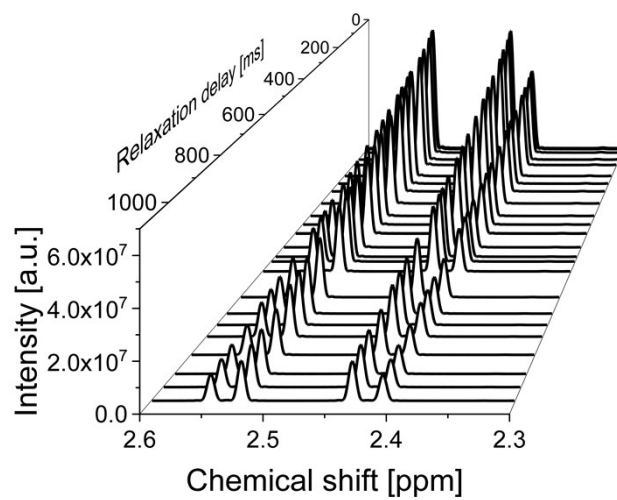


**Figure S10.** Typical CPMG experiment with the decrease of the 2.38 ppm signal intensity of trisodium citrate tracked by the relaxation delay at 22 °C.

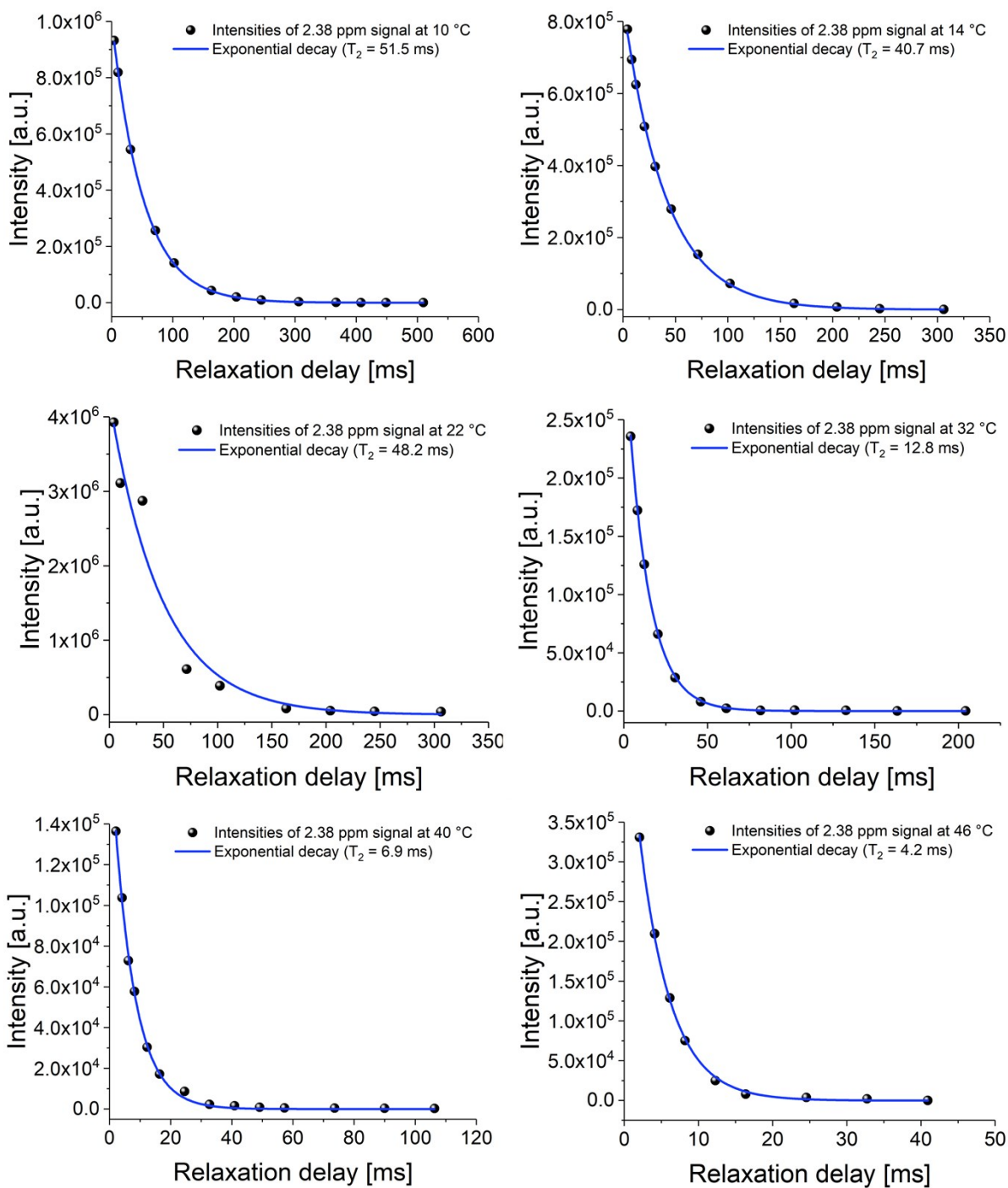


**Figure S11.** Intensity of the  $\text{Ni}^{2+}$ -citrate  $^1\text{H}$ -NMR signal as a function of the relaxation delay during CPMG experiments conducted at 10 °C, 14 °C, 22 °C, 32 °C, 40 °C and 46 °C. Data is fitted with a standard exponential decay function to obtain  $T_2$  (blue line).

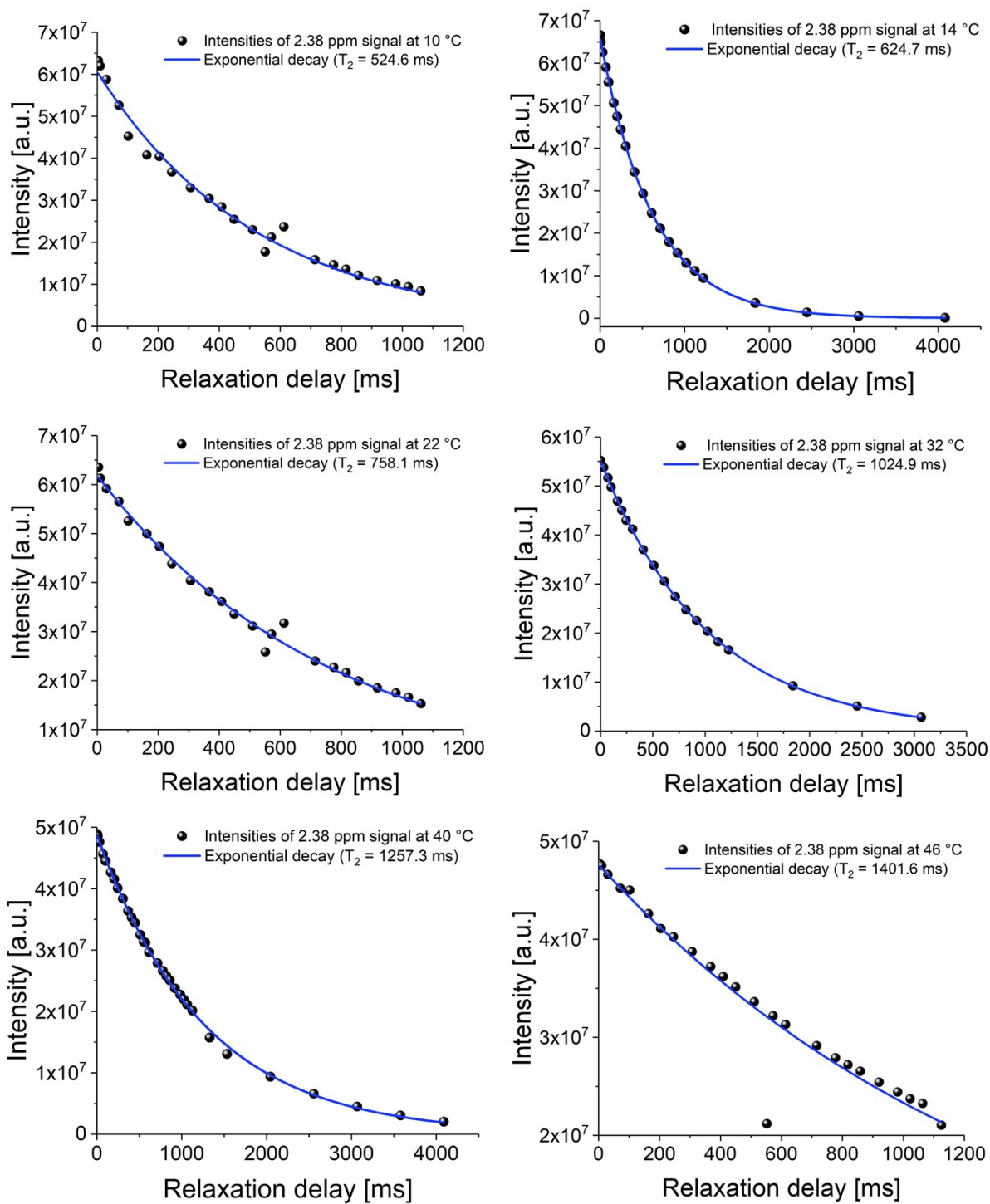


**Figure S12.** Intensity of the citrate <sup>1</sup>H-NMR signal as a function of the relaxation delay during CPMG experiments conducted at 10 °C, 14 °C, 22 °C, 32 °C, 40 °C and 46 °C. Data is fitted with a standard exponential decay function to obtain T<sub>2</sub> (blue line).

The obtained data is fitted by standard exponential decay:

$$y = A \cdot e^{-\frac{x}{T_2}} \quad (1)$$

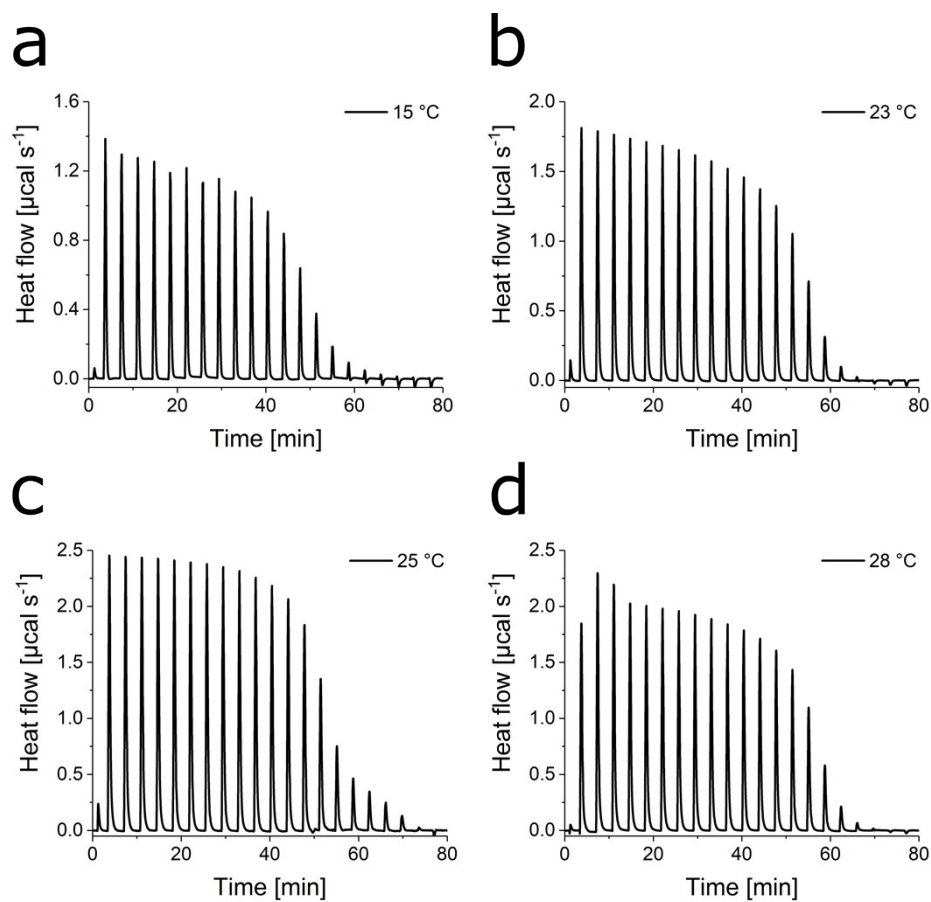


**Figure S13.** Thermograms of the Ni<sup>2+</sup>-citrate complexation at different temperatures (15 °C, 23 °C, 25 °C and 28 °C) obtained via ITC.

## 8. Additional references

1. A. Kumar and S. Bhattacharyya, *ACS Appl. Mater. Interfaces*, 2017.
2. B. Folch, Y. Guari, J. Larionova, C. Luna, C. Sangregorio, C. Innocenti, A. Caneschi and C. Guérin, *New J. Chem.*, 2008, **32**, 273-282.